THE JOURNAL OF PHYSICAL CHEMISTRY C
A JOURNAL OF THE AMERICAN CHEMICAL SOCIETY

pubs.acs.org/JPCC Article

Recoverability of N_4^{x-} Anions to Ambient Pressure: A First-Principles Study of *cyclo*- and *syn*-Tetranitrogen Units

Sergey V. Bondarchuk*

Cite This: *J. Phys. Chem. C* 2021, 125, 7368−7377 Read Online

ABSTRACT: In this paper, we have analyzed the possibility of various neutral and anionic forms of both cyclic and acyclic N_4 species to be recovered to ambient conditions using state-of-the-art computational techniques. Phonon dispersion and mechanical properties calculations as well as *ab initio* molecular dynamics simulations revealed that *syn*-tetranitrogen units are kinetically stable only in the form of N_4^{4-} anion. Meanwhile, salts of cyclic N_4 (*c*-N_4, tetrazete) with alkali, alkaline earth metals, and aluminum appeared to be dramatically stable at ambient conditions for a wide range of oxidation states of *c*-N_4^{x-} from x = 1−3. Varying both metal and stoichiometry, one can obtain salts with a wide range of properties: band gap (1−5 eV), bulk modulus (36−196 GPa), enthalpy of formation (from −21 to 660 kJ mol^{-1}), and so forth. Thus, crystal structure prediction and comprehensive characterization, which included bonding nature, stability criteria, spectral properties along with thermodynamic and energetic characteristics of *c*-N_4 and its salts (Na_2N_8, Li_2N_4, MgN_4, and AlN_4) as well as calcium salt of *syn*-N_4^{4-} (Ca_2N_4) are performed in this work. The obtained results significantly expand our understanding of the possible forms of nitrogen existence in nature, which, if synthesized, can find a number of interesting applications.

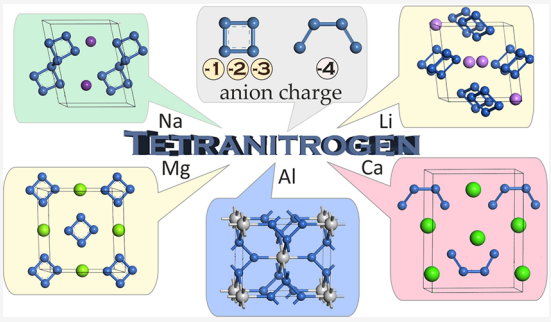

1. INTRODUCTION

Dinitrogen is the most abundant gas in the Earth's atmosphere. Having an extremely robust molecule, N≡N is a chemically inert compound, and its name originates from "azōos", Greek for "lifeless". In this regard, it is remarkable to realize that nitrogen, in fact, is an essential part of living matter, and it forms a variety of minerals and chemical compounds, both organic and inorganic. It becomes obvious that a huge quantity of energy is needed to transform dinitrogen into other compounds bearing the N═N or N—N bonds. But this expense of energy is justified since one may obtain a nitrogen-rich high-energy density material (HEDM), which has a number of advantages compared to a conventional HEDM, namely, environmentally friendly gaseous products and high detonation/propulsive characteristics (heat of formation, explosive power, specific impulse, flame temperature, etc.).[1]

This is the reason why a growing number of new unique forms of nitrogen are obtained experimentally:[2] cg-N,[3] LP-N,[4] HLP-N,[5] −$(NH)_n$−,[6] $ReN_8 \cdot xN_2$,[7] N_8,[8] N_8^-,[9] and *cyclo*-N_5^-.[10−12] All of these materials, except of the latter two anions, survive only at extreme pressures (tens to hundreds of gigapascals), but encapsulation of cg-N into a carbon nanotube allowed one to obtain even such a polymeric form of nitrogen at near ambient conditions.[13] Therefore, this gives a reason to hope for a successful synthesis of other predicted nitrogen allotropes, in particular, bipentazole N_{10},[14,15] which has the lowest enthalpy among all of the other nitrogen allotropes in the pressure range of 0−42 GPa.[14] Moreover, it is known that two the lowest-energy allotropes, cg-N and N_8, were first predicted using first-principles calculations[16,17] and then obtained experimentally. For a more detailed review of the predicted forms of nitrogen, please refer to the recent papers.[18−21]

Concerning the study of the tetranitrogen (N_4) unit, it can be divided into the period before and after the development of methods for predicting crystalline structures. Before such algorithms, the proposed forms of N_4 were cyclic (D_{2h}-N_4), tetrahedral (T_d-N_4), various acyclic forms, radical cations ($N_4^{\bullet+}$), dications (N_4^{2+}), and so forth.[22−28] The interest in this topic was restored within the latter five years, when a number of various forms of nitrogen binary compounds were predicted under a wide pressure range. Thus, using evolutionary (USPEX) or particle swarm optimization (CALYPSO) algorithms, the following forms of N_4 were predicted at high pressures: *anti*-N_4^{4-} anion in CsN,[29] CaN_2[30] and BaN_2;[31] *catena*-N_4^{2-} in LiN_2[32] and three-pointed stars D_{3h}-$N(N)_3^{4-}$ in MgN_2.[33] Two great recent discoveries, however, have only partially confirmed these calculations. Indeed, within the diamond anvil cell (DAC) experiments, the *catena*-N_4^{2-}

Received: December 23, 2020
Revised: March 10, 2021
Published: March 25, 2021

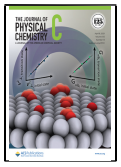

https://doi.org/10.1021/acs.jpcc.0c11425
J. Phys. Chem. C 2021, 125, 7368−7377

polyanions were detected in FeN_4 at high pressures. On the other hand, discovery of *syn*-N_4^{4-} anions at ambient pressure in the form of Mg_2N_4 was a real surprise.[22,23] This makes us take a completely new look at the possible forms of nitrogen in nature, especially at the cyclic N_4 form, whose anions are expected to be more thermodynamically stable than that of the open chain forms (Chart 1).

Chart 1. Resonance Structures of Various Anions of Cyclic and Acyclic Form of N_4[a]

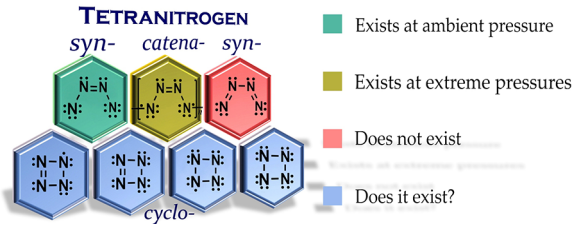

[a]Lone pairs and unpaired electrons are marked with dots.

Indeed, the corresponding *syn*-N_4^{2-} anion has intrinsic instability with respect to the N2—N3 bond, which is clearly seen from its resonance structure (Chart 1) and decomposes into the N_2^- species. This is the reason why it was obtained only in the form of a *catena*-polyanion (Chart 1) having the N2═N3 bond and only at high pressures as a ferrous salt with a formal unit FeN_4.[35] As our preliminary calculations showed, all acyclic anions, including *syn*-N_4^{4-}, are unstable in the gas phase; the same picture is characteristic for the anions of T_d-N_4. Conversely, the anions of *cyclo*-N_4 (with anion charges −1, −2, −3, and −4) are all stable in the gas phase.

Thus, in this work, we have tried to find out if these cyclic anions could form metal salts that are stable at ambient conditions. For this purpose, we have applied state-of-the-art computational methods which were aimed at crystal structure prediction and checking dynamical, mechanical, and thermal stability of the latter species at ambient conditions. These stability criteria were recently put forward as a good "screen" for new predicted materials.[36] Of course, for a precise crystal structure prediction one needs to obtain a convex hull as well as to be sure that all of the potential energy landscape is scanned.[37] But this still does not guarantee that the predicted structure is the lowest energy one, but instead may be a higher energy polymorph. For example, high- and low-pressure Mg_xN_y crystal structures, which were recently predicted by means of the USPEX method utilizing a sophisticated evolutionary algorithm[33] do not match with the experimentally obtained ones using DAC experiments.[34] On the other hand, the prediction of a metastable *catena*-MgN_4 polymorph at high pressure (*Cmmm*)[33] means that its thermodynamically stable form (*Ibam*) can exist at given conditions and can be synthesized.[34]

2. COMPUTATIONAL DETAILS

Crystal structure predictions were performed using Polymorph module of the Materials Studio 2017 program suite.[38] All anions were first optimized using the DFT(ωB97XD)/6-31+G(d,p) method[39,40] and their Merz−Kollman electrostatic potential fitting partial charges were obtained. These calculations were performed using the Gaussian09 program package.[41] The obtained partial charges were then applied for the structure prediction using the Polymorph module. This procedure includes four steps: (a) simulated annealing, during which thousands of crystal structures are built and randomly modified; (b) clustering when all available frames for the specified space groups are clustered; (c) geometry optimization with rigid body constraints using the Universal force field[42] (thus, only interionic interactions were relaxed at this step); (d) final clustering. The crystal structure prediction was performed for seven of the most frequent space groups, which are the following: $P2_1/c$ (34.3%), $P\bar{1}$ (25.0%), $C2/c$ (8.3%), $P2_12_12_1$ (7.0%), $P2_1$ (5.1%), *Pbca* (3.3%), and $Pna2_1$ (1.4%).[43] Thereafter, the lowest-energy crystals were treated according to our recently proposed vibrational eigenvector-following scheme.[44,45] In total, these seven space groups cover 84.4% of all crystal structures in Cambridge Structural Database. Moreover, inclusion of the high-symmetry crystal systems (cubic, hexagonal, etc.) is absolutely unlikely in the case of a D_{2h}, D_{4h}, or C_{2v} molecular system plus metal atom(s), especially since the eigenvector-following scheme allows transition to another space group expanding the search boundaries.

According to this scheme, crystals obtained with the Polymorph were completely relaxed using Cambridge Serial Total Energy Package (CASTEP) code[46] implemented in the Materials Studio 2017 program suite.[38] Norm-conserving (NC) pseudopotentials with the states H-$1s^1$, N-$2s^22p^3$, Li-$2s^1$, Na-$2s^22p^63s^1$, K-$3s^23p^64s^1$, Mg-$2s^22p^63s^2$, Al-$3s^23p^1$, Ca-$3s^23p^64s^2$, Cl-$3s^23p^5$, and Br-$4s^24p^5$ treated as the valence electrons were applied entirely in this work. Cell relaxations, phonons, elastic constants, spectral and energetic properties calculations, as well as molecular dynamics simulations were performed using pure GGA functional due to Perdew−Burke−Ernzerhof (PBE),[47] whereas the band structure calculations were done with a much more expensive, but more accurate hybrid exchange-correlation functional HSE06.[48]

Wave functions were expanded in a plane wave basis set with an energy cutoff, which depends on the convergence test for each element.[38] These are the following: H (720 eV), N (770 eV), Li (500 eV), Na (770 eV), K (440 eV), Mg (990 eV), Ca (880 eV), Cl (830 eV), and Br (280 eV). Thus, for any combination of these elements the energy cutoff was determined by the highest value. For the band structure calculations, however, a basis set cutoff of 700 eV was applied for all of the crystals as a reasonable compromise between computational cost and accuracy.[19,49] Sampling of the Brillouin zones were performed using *k*-point grids generated by the Monkhorst−Pack algorithm. Direct spacing between *k*-points was specified to 0.08 2πÅ^{-1} for all of the calculations. Convergence criterion of the total energy was set to 5×10^{-6} eV atom^{-1}. For a more correct prediction of the enthalpies of formation, dispersion effects were taken into account using the Grimme form of the damped C_6 term.[50] These play an important role in the considered metal−nitrogen salts; for example, in AlN_4 the dispersion forces equal 121.6 kJ mol^{-1}.

The DMol^3 calculations were performed within the all-electron approximation along with the PBE functional and the double numerical basis set DND (basis file version 3.5).[51] The DMol^3 code allows calculation of both periodic and nonperiodic structures without application of the supercell approximation, which significantly speed up the calculation. Topological analysis of the electron density distribution in real space (QTAIM) was performed using AIMQB program within the AIMStudio suite using the Proaim basin integration method.[52] For this purpose, 3 × 3 × 3 supercells (the Rubik's cube form) were built and transformed into nonperiodic structures. Thereafter, the corresponding wave functions were obtained

https://doi.org/10.1021/acs.jpcc.0c11425
J. Phys. Chem. C 2021, 125, 7368−7377

for the whole cubes on the basis of the DFT(ωB97XD)/6-31+G(d,p) calculations, but the QTAIM properties were analyzed only for inner asymmetric cells. Such an approach allows taking into account all possible interactions of the inner asymmetric cells with neighbors.

3. RESULTS AND DISCUSSION

3.1. Structure and Stability. First of all, we have tried to check whether parent tetrazete (c-N_4) is kinetically stable in the crystalline environment. As a result, we have obtained a tetragonal crystal of the $P4_2/mnm$ space group (Figure S1a in the Supporting Information). Indeed, c-N_4 forms D_{2h}-symmetric molecules with two stretched bonds (1.546 Å). This is much higher than the N—N bond length in hydrazine (1.459 Å), therefore c-N_4 is expected to have a small thermal stability. Moreover, its relative enthalpy is very high and even exceeds that of polymeric nitrogen cg-N (140.1 kJ mol^{-1} atom^{-1})[14] at ambient pressure (Figure S1b in the Supporting Information). At 50 GPa, c-N_4 is still far from α-N_2, although the latter is no longer the lowest energy allotrope. Nevertheless, c-N_4 demonstrates dynamical and mechanical stability at 0 K, which can be seen from the corresponding phonon dispersion and the 3D Young modulus; however, at finite temperatures, at least 200 K, this forms two isomeric N_8 structures, namely, 1-tetrazetyltetraaza-1,3-diene and 1,2-diazidodiazene, which is following from our *ab initio* molecular dynamics simulations (Figure 1c−e in the Supporting Information). It is interesting

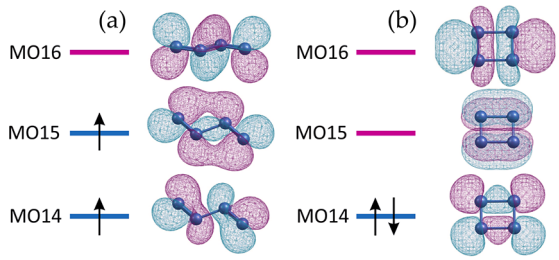

Figure 1. Frontier molecular orbitals of acyclic (a) and cyclic (b) neutral N_4 unit.

that the latter isomer was recently detected experimentally at 3 GPa.[8] Thus, such high enthalpy of formation along with its weak N—N bonds makes synthesizability of c-N_4 extremely hard.

As we have mentioned above, acyclic N_4^{2-} has intrinsic instability with respect to the N(2)—N(3) bond (Chart 1). This also can be easily seen from the corresponding frontier molecular orbitals (MO) of the C_2h-N_4 (Figure 1a). As one can see, it has the triplet ground state, while the singlet state is kinetically unstable. This is clearly seen from the antibonding character of MO14 with respect to the N(2)—N(3) bond. The same situation is for the reduced (anionic) form of C_{2h}-N_4, when only highly reduced forms C_{2h}-N_4^{3-} and C_{2h}-N_4^{4-} (occupied MO16) are expected to be kinetically stable. The calculations show, however, that only the C_{2h}- and C_{2v}-N_4^{4-} anions appear to be stable. Conversely, the cyclic form (D_{2h}-N_4) appears to be stable in the singlet ground state due to a bonding character of MO14 with respect to the N(2)—N(3) bond and in oxidation states from −1 to −2 since one- and two-electron reduction of D_{2h}-N_4 leads to occupation of MO15, which has a bonding character with respect to the stretched bonds (Figure 1b). Further reduction to D_{2h}-N_4^{3-} put an electron on MO16 with an antibonding character with respect to the stretched bonds, but it is still not enough to break them; thus, D_{2h}-N_4^{3-} anion is expected to be also stable. Finally, in D_{2h}-N_4^{4-} the MO16 is doubly occupied; this means instability of a planar structure, which distorts to the out-of-plane D_{2d}-N_4^{4-} structure, weakening the overlap of the 2p electrons.

To check these arguments in practice, we have tried to compare relative energies of acyclic and cyclic anions in crystalline state. For this purpose, we have predicted crystal structures of NaN_4, MgN_4, AlN_4 and Mg_2N_4 in the $P1$ space group neglecting the energy differences between possible polymorphs, which usually do not exceed 2 kJ mol^{-1} for molecular crystals.[53] As we have recently shown for RDX, within a 1% error for D the error of prediction of d_c and ΔH_f can be varied in the ranges of −1.4−1.4 and −220.2−42.0%, respectively. Similarly, for P these ranges are −0.5−0.5 and −53.0−26.4%, respectively.[54] The calculations completely confirm instability of the acyclic N_4^-, N_4^{2-}, and N_4^{3-} forms, which decompose due to breaking of the N2—N3 bond. Conversely, the cyclic N_4^{4-} anion appears to be more energetic than the acyclic form despite the distortion of the cycle (out-of-plane D_{2d} symmetry), which prevents unfavorable conjugation of 8 π-electrons. This completely agrees with the available experimental data on Mg_2N_4 ($P2_1/n$).[34]

Thus, in this work we have varied both the metal and the anionic charge (stoichiometry) to check accessibility of the c-N_4^-, c-N_4^{2-}, c-N_4^{3-}, and syn-N_4^{4-} anions as well as various metals (Li, Na, Mg, Al, and Ca) as cationic components. As a result, we have obtained salts for all the anions, except of c-N_4^-, for which recombination of the radical anions takes place at high temperatures (600 K) with the subsequent formation of a dianion N_8^{2-}, in which a c-N_4 moiety possesses formal charge −1 (Figure 2, Na_2N_8). Meanwhile, NaN_4 is also dynamically and mechanically stable and probably can exist at low temperatures; therefore, we also report the calculated data for this salt (Figure S2 in the Supporting Information). We should also stress that c-N_4^- and c-N_4^{3-} possess odd numbers of electrons; therefore, their salts may demonstrate ferromagnetic or antiferromagnetic properties.

In the salts of c-N_4, anions have point group symmetry C_i (Na_2N_8), D_{2h} (Li_2N_4), and D_{4h} (MgN_4 and AlN_4). However, in the first two cases the symmetry is very close to C_{2h} and D_{4h}, respectively. Bond lengths vary from 1.358 to 1.461 Å, but in the oxidation state −2, the bond lengths are distributed more uniformly and are slightly shorter (Figure 2). In the case of Ca_2N_4, the calculated parameters of the syn-N_4^{4-} anion appear to be close to ones experimentally obtained for α-Mg_2N_4: N1−N2 (1.357 versus 1.388 Å), N2−N3 (1.330 versus 1.325 Å), and ∠N1−N2−N3 (120° in both cases).[34] Different projections of a 4 × 4 × 4 slab for the studied crystals are illustrated in Figure S3, and the corresponding fractional coordinates are listed in Table S1 in the Supporting Information.

An interesting question arises about the nature of bonding in such salts. In particular, it is interesting if the N_4^{x-} species form ionic bonds with the cations or, probably, coordination or even covalent bonds. For this purpose, we have performed a Quantum Theory of Atoms in Molecules (QTAIM) analysis. In Table 1, the $\nabla^2\rho(\mathbf{r})$ and $h_e(\mathbf{r})$ values correspond to the critical point of the shortest metal−N distance (see Figure S4 in the Supporting Information) and the $g(\mathbf{r})$ values correspond to the N_4 ring critical point. The nature of bonding was analyzed in accord with the Cremer−Kraka criteria,[55] which can be effectively applied even in stretched or dissociative systems.[56] It is seen in Table 1 that $\rho(\mathbf{r})$ at the metal−N bond critical points

https://doi.org/10.1021/acs.jpcc.0c11425
J. Phys. Chem. C 2021, 125, 7368−7377

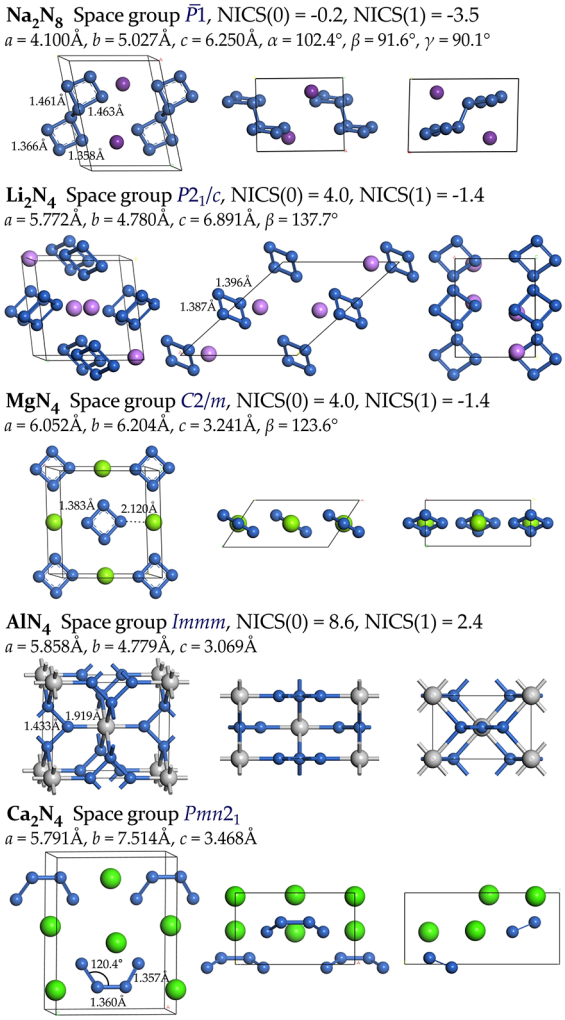

Figure 2. Optimized asymmetric cells of the studied salts.

Table 1. Selected QTAIM Properties (in 10^3 au) and Cationic Charges (q_M in e^-)

entry	$\rho(\mathbf{r})$	$\nabla^2\rho(\mathbf{r})$	$h_e(\mathbf{r})$	$g(\mathbf{r})$	q_M
Na_2N_8	13.273	68.960	2.936	199.346	0.978
Li_2N_4	22.484	146.654	7.748	226.290	0.886
MgN_4	37.416	244.915	8.541	220.625	1.631
AlN_4	62.385	421.103	3.915	179.090	2.918
Ca_2N_4	34.573	189.033	4.388		1.430

in all of the salts is lower than 0.1 au; moreover, the $\nabla^2\rho(\mathbf{r})$ values are all positive. This indicates the metal−N bonds as closed shell interactions. Finally, the positive values of $h_e(\mathbf{r})$ specify these interactions as ionic, rather than coordination. This is also reflected in the values of the QTAIM charges on the metal cations (q_M). On the other hand, the metal−N bond in AlN_4 is close to that of AlN (1.885−1.915 Å)[57] in length and, obviously, in nature. It is known that the latter is partially covalent but, nevertheless, has essentially ionic character.[58] The QTAIM analysis of AlN also suggests a strong similarity of these bonds.

Surprisingly, as it follows from the corresponding values of nucleus-independent chemical shifts (NICS) in Figure 2, aromatic character of N_4^{2-} is very weak. For example, despite formal 6p electrons in the π-system of N_4^{2-}, the corresponding NICS(1) is close to zero. Conversely, σ-aromaticity is higher, which was also found in the case of in-plane bishomoaromaticity of specifically preoriented bisdiazenes forming cyclic tetranitrogen dianions.[59] It is also interesting to estimate ring strain energies (RSE) of the N_4^{x-} rings. Qualitatively, this may be done using the known direct dependence between RSE and $g(\mathbf{r})$ in the corresponding ring critical point.[60] Among the studied salts, AlN_4 has the lowest ring strain, while Li_2N_4 has the highest one, which is caused by the shorter N—N bonds in the latter. More information can be obtained by comparing $g(\mathbf{r})$ of these salts with ones for other nitrogen cycles known experimentally. Thus, we have calculated $g(\mathbf{r})$ for N_5^- ring in potassium pentazolate[61] (0.13332 au), N_3 ring in ethyl 2,3-diisopropyltriaziridine-1-carboxylate[62] (0.26314 au), and $N_4^{\bullet+}$ ring in tetraisopropyl tetrazetidine-1,2,3,4-tetracarboxylate radical cation[63] (0.20358 au). Thus, one can conclude that RSE in the studied metal salts should occupy an intermediate position between the synthetically available five- and three-membered nitrogen cycles and does not cause excessive destabilizing effect.

As in the case of the parent tetrazete, we have performed a series of calculations to check dynamical, mechanical, and thermal stability of the above-described salts; the results are presented in Figures 3 and 4. Note that the Brillouin zone integrations were performed within the standardized high-throughput approach which offers the standard integration paths for all the 24 Brillouin zones (the corresponding paths are illustrated in Figure S5 in the Supporting Information).[64] As one can see in Figure 3, all salts are dynamically stable and demonstrate no soft modes in the phonon spectra. Moreover, all salts are mechanically stable, which can be seen from the positive values of the Young modulus in whole 3D space (Figure 3).

To check mechanical stability, we have calculated elastic constants using energy versus strain method. Thereafter, the mechanical stability was examined according to the Born−Huang criteria for the 11 Laue classes.[65] For all stable materials, the corresponding 3D plots of the Young modulus were built on the basis of the elastic compliance constants (Tables S2 and S3 in the Supporting Information).[66] For polycrystalline materials, the corresponding bulk moduli (K) are illustrated in Figure 3 and other mechanical properties, Lamé parameters (μ and λ), Young modulus (E), and Poisson ratio (ν) in the Hill approximation, are gathered in Table 2. It is clear that all salts are mechanically hard materials since their bulk moduli are higher than typical values for molecular crystals and metal salts.[67,68] In particular, AlN_4 demonstrates very high K and E values which are close to that of AlN (K = 202.7 GPa and E = 336.1 GPa).

Finally, we have checked thermal stability of the studied materials by means of *ab initio* molecular dynamics simulations. For this purpose, we have built the corresponding supercells being 1 × 2 × 2 slabs of the corresponding asymmetric cells. Thus, these simulations were performed with the NVT ensemble at 600 K, which should be enough for justification of thermal stability at ambient temperature. Time step was 1 fs and the total simulation time was 10 ps (Figure 4). As one can see, no substantial rise of temperature or constant of motion was observed. Temperature fluctuates uniformly and constant of motion slowly increases. Moreover, all N_4^{x-} rings remain unbroken and any decomposition was not observed.

3.2. Spectral and Energetic Properties. To facilitate spectral identification of the studied compounds, we have calculated their IR and Raman spectra (Figure S6 in the Supporting Information). All salts of c-N_4, except for Na_2N_8, anions demonstrate a triplet of the IR bands and a doublet of the Raman bands, which vary within the range of about 200−600

https://doi.org/10.1021/acs.jpcc.0c11425
J. Phys. Chem. C 2021, 125, 7368−7377

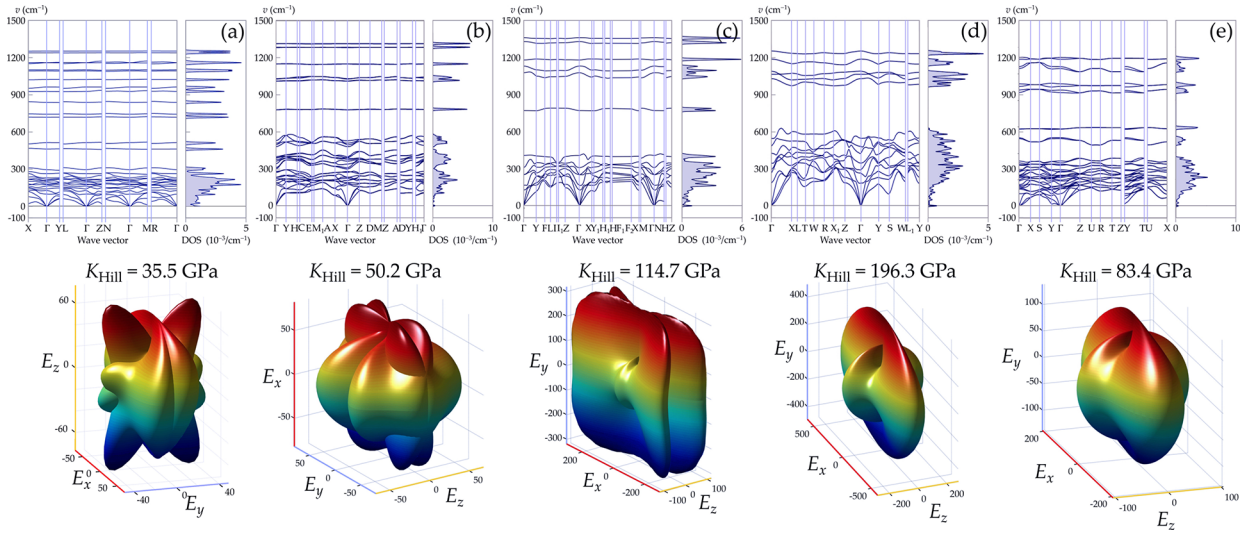

Figure 3. Calculated phonon dispersions and 3D maps of the Young modulus of the studied salts.

and 1150−1300 cm^{-1}, respectively. Meanwhile, Na_2N_8 has a doublet of the IR intense bands at about 200 cm^{-1} and a single intense band at 1150 cm^{-1}. In the Raman spectrum, Na_2N_8 demonstrates an intense band at about 1250 cm^{-1}. The spectra of Ca_2N_4 have a somewhat different pattern, which is characterized by the presence of the IR intense bands at about 820 and 1020 cm^{-1} and a Raman active band at about 880 cm^{-1}.

Also, we have calculated band structures for the studied materials, and the corresponding plots are presented in Figure S7 in the Supporting Information. It is interesting that the band gap values vary from 0.948 to 5.206 eV (Table S4 in the Supporting Information). Thus, AlN_4 is expected to be a direct band gap semiconductor (ΔE_{gap} = 0.946 eV). At the same time, Na_2N_8, MgN_4, and Ca_2N_4 demonstrate indirect band gaps of 3.905, 3.687, and 2.442 eV, respectively, and can be characterized as wide band gap semiconductors. Finally, Li_2N_4 is a typical insulator with an indirect band gap of 5.206 eV. Thus, by varying stoichiometry and the nature of metal one can obtain a wide spectrum of electronic properties of the tetranitrogen anion salts.

A very important question about the nature of the studied salts concerns their enthalpies of formation and accompanying energetic properties (detonation, propulsive). The latter must be calculated with a maximum accuracy and compared with the similar properties for other experimentally known forms of nitrogen, azides, and pentazolates. Thus, we have started from calibration of our calculation method. In this work, we have applied two approaches for the prediction of ΔH^0_{solid}.

The first approach is based on the estimation of both the gas-phase enthalpy (ΔH^0_{gas}) and sublimation enthalpy (ΔH_{sub})

$$\Delta H^0_{gas} = E_X - \sum nE_{atom} \quad (1)$$

$$\Delta H_{sub} = -\frac{E_{solid}}{Z'} + E_{gas} - 2RT \quad (2)$$

where E_X and E_{atom} are the zero-point corrected total energies of a given compound and its constituting elements in their stationary states (in Ha), and n is the stoichiometric index of each atom in the molecule; E_{solid} and E_{gas} are the total energies of the studied molecule in its crystalline form and in vacuum (in eV); R and T are the gas constant and absolute temperature. Thus, the solid-state enthalpy is easily calculated as in eq 3

$$\Delta H^0_{solid} = \Delta H^0_{gas} - \Delta H_{sub} \quad (3)$$

In this method, E_{atom} are obtained by the least-squares fitting of the calculated and experimental gas-phase enthalpies.[45,66] Species included in the benchmark set in this work are listed in Table S5 in the Supporting Information and their experimental values are taken from the NIST Chemistry WebBook.[69] Thus, the obtained E_{atom} values are listed in Table 3.

As one can see in Table S5, this method demonstrates a rather accurate prediction of both ΔH^0_{gas} and ΔH_{sub} for all compounds with known gas-phase and solid-state enthalpies of formation. Also, we have checked this approach for NH_4Cl and metal azides for which only ΔH^0_{solid} is known experimentally.[70] Again, this method reproduces the latter values rather accurately. Finally, we have tried to predict ΔH^0_{solid} for potassium pentazolate (KN_5), for which this value was estimated to be 136.8 kJ mol^{-1}.[71] In the present work, we predict this enthalpy of formation to be 101.2 kJ mol^{-1}. Thus, the calculated enthalpies for c-N_4 and its salts are listed in Table 4.

As one can see, eq 3 fails in the prediction of ΔH^0_{solid} for Ca_2N_4, since syn-N_4^{4-} anion is unstable in the gas phase. Thus, we have developed another method for a direct estimation of ΔH^0_{solid} using the corrected atomic energies E_{atom}

$$\Delta H^0_{solid} = E_X - \sum nE_{atom} \quad (4)$$

The corrected DMol^3 atomic energies E_{atom} are listed in Table 3 and the calculated enthalpies of formation are presented in Table S6 in the Supporting Information. Such an approach is very simple and convenient because it allows a direct estimation of the solid-state enthalpy of formation using a simple cell relaxation. However, it provides some divergence with the previous method, in particular for magnesium and aluminum containing crystals. This is obviously due to a too small benchmark set, and an extension of which should significantly improve the results.

Thus, the calculated solid-state enthalpies of formation of all the studied compounds are presented in Table 4. As one can see, the ΔH^0_{solid} values are scattered a lot; Li_2N_4 and Ca_2N_4 have negative enthalpies and the other salts have positive ones being in the same range as that of most energetic materials. We have also estimated ΔH^0_{solid} for Ca_2N_4 using the enthalpy of the

https://doi.org/10.1021/acs.jpcc.0c11425
J. Phys. Chem. C 2021, 125, 7368−7377

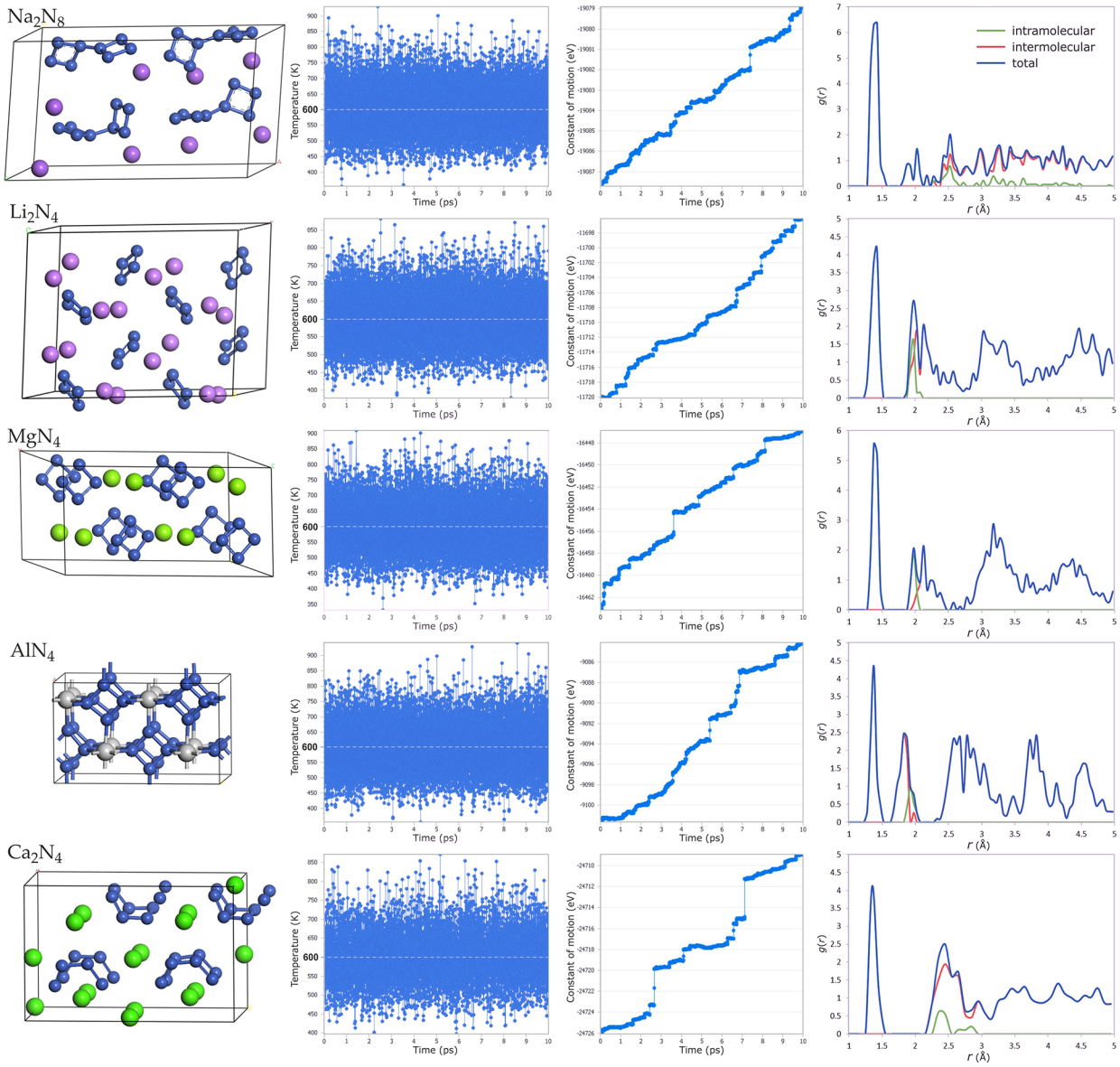

Figure 4. Results of the *ab initio* molecular dynamics simulations. From left to right: snapshot of the final geometry, temperature, constant of motion, and radial distribution function.

Table 2. Calculated Mechanical Properties of the Studied Compounds in the Forms of Polycrystalline Materials

entry	μ	λ	E	ν
Na_2N_8	16.7	24.2	43.2	0.29607
Li_2N_4	25.0	33.5	64.4	0.28635
MgN_4	70.7	67.6	175.9	0.24440
AlN_4	120.7	115.9	300.5	0.24490
Ca_2N_4	46.3	52.5	117.3	0.26558

following reaction: $Ca_2N_4 = 2Ca_{(s)} + 2N_{2(g)}$. This value is close to the one calculated using eq 4, −170.2 versus −172.3 kJ mol^{-1}, respectively.

Table 4. Calculated Gas Phase and Solid State Enthalpies of Formation and Sublimation

entry	ΔH^0_{gas}	ΔH_{sub}	$\Delta H^0_{solid\ (eq\ 3)}$	$\Delta H^0_{solid\ (eq\ 4)}$
Na_2N_8	980.9	321.4	659.5	660.2
Li_2N_4	452.2	473.0	−20.8	11.9
MgN_4	780.4	624.1	156.3	86.1
AlN_4	760.6	464.4	296.2	362.4
Ca_2N_4				−172.3

Having the values of solid-state enthalpies of formation, we have calculated detonation properties of the studied compounds, namely, detonation energy (Q), velocity (D), and

Table 3. Atomic Energies E_{atom} (in Ha) applied in Equation 1 and Equation 4 for Calculation of Enthalpies of Formation

method	Li	Na	K	Mg	Ca	Al	H	N	Cl	Br
eq 1	−7.5363	−162.2883	−599.8961	−200.0732	−677.5379	−242.4343	−0.5801	−54.7512	−460.1706	−2571.7554
eq 4	−7.5273	−162.2201	−599.7441	−199.9975	−677.3644	−242.3593	−0.5854	−54.7363	−460.0181	−2573.8301

https://doi.org/10.1021/acs.jpcc.0c11425
J. Phys. Chem. C 2021, 125, 7368−7377

Table 5. Equilibrium Detonation Patterns and the Calculated Detonation Properties of the Studied Compounds

entry	equilibrium composition of the detonation products	ρ (g cm^{-3})	Q (cal g^{-1})	D (m s^{-1})	P (GPa)
Na_2N_8	0.6688 $N_{2(g)}$ + 0.22449 $Na_{(g)}$ + 0.00321 $Na_{2(g)}$ + 0.10350 $Na_{(l)}$	2.088	960.22	3566	6.11
MgN_4	0.82925 $N_{2(g)}$ + 0.16259 $Mg_3N_{2(cr)}$ + 0.00816 $Mg_{(cr)}$	2.633	688.18	5840.2	18.38
AlN_4	0.60537 $N_{2(g)}$ + 0.36781 $AlN_{(l)}$ + 0.02682 $Al_{(g)}$	3.210	1165.20	6373.2	23.76

pressure (P). For this purpose, we applied the Kamlet−Jacobs empirical scheme. Being originally proposed for CHNO explosives, this was extended to various metal-containing compounds.[72] Within this scheme, Q can be expressed as the following

$$Q = -\frac{\left(\sum n\Delta H_f^P\right) - \Delta H_f^X}{\mathrm{MW}} \tag{5}$$

where ΔH_f^X and ΔH_f^P are enthalpies of formation of the given explosive X and its detonation products P, scaled by their mole fractions n; MW is the molecular weight of X.

To determine D and P, one needs to calculate moles of detonation gases per gram of explosive (N), and average molecular weight of detonation gases ($\bar{M}$)

$$N = \frac{1}{\mathrm{MW}} \sum_i n_i \tag{6}$$

$$\bar{M} = \frac{\sum_{i=1}^{NS} n_i \mathrm{MW}_i}{\sum_{i=1}^{NG} n_i}\left(1 - \sum_{i=NG+1}^{NS} k_i\right) \tag{7}$$

Herein, n_i is the mole fractions of gases; k_i is the mole fractions of condensed species. Note, the indexes NG and NS correspond to gases and total number of species in the mixture. Thus, gases are indexed from 1 to NG and condensed species from NG+1 to NS.[73]

For accurate estimation of the above-mentioned quantities, the equilibrium composition of the detonation products must be obtained. For this purpose, we have defined new reactants for the NASA CEA2 program[73] using the temperature dependence of the main thermodynamic functions (Figure S8 in the Supporting Information) obtained with CASTEP. Using previously described procedures,[74] these data were converted into the NASA 9 coefficients as the least-square fit coefficients (a_1...a_9) for the polynomials of the following forms[75]

$$\frac{C_p^\circ}{R} = a_1T^{-2} + a_2T^{-1} + a_3 + a_4T + a_5T^2 + a_6T^3 + a_7T^4 \tag{8}$$

$$\frac{H^\circ}{RT} = -a_1T^{-2} + a_2T^{-1} + \ln T + a_3 + a_4\frac{T}{2} + a_5\frac{T^2}{3} + a_6\frac{T^3}{4} + a_7\frac{T^4}{5} + \frac{a_8}{T} \tag{9}$$

$$\frac{S^\circ}{R} = -a_1\frac{T^{-2}}{2} - a_2T^{-1} + a_3 \ln T + a_4T + a_5\frac{T^2}{2} + a_6\frac{T^3}{3} + a_7\frac{T^4}{4} + a_9 \tag{10}$$

These coefficients are presented in the Supporting Information. Thus, the calculated equilibrium compositions of the detonation products are listed in Table 5. The entries for Li_2N_4 and Ca_2N_4 are missing since these salts have negative Q and are not explosive. All of the remaining salts demonstrate lower performance compared to conventional CHNO explosives, which is attributed mainly to their low detonation energies.

To check the accuracy of the Kamlet−Jacobs scheme, we have used metal azides as the most relevant metal−nitrogen systems for which experimental data on detonation velocities are present. We have found in the literature the D values for $Pb(N_3)_2$, AgN_3, and $Cu(N_3)_2$ and the corresponding calculations using one of the most popular commercial software Explo5.[76] The corresponding input data and the results are presented in Tables S7 and S8 in the Supporting Information. As one can see, the Kamlet−Jacobs scheme provides results which are comparable with that of Explo5 software. Thus, the predicted detonation velocity is underestimated (11.1 and 25.3%) and overestimated (28.3%) for $Pb(N_3)_2$, $Cu(N_3)_2$ and AgN_3, respectively.

Finally, we have calculated propulsive properties of the positive detonation energy salts as monopropellants in terms of the finite-area combustor (FAC) approximation[73] (Table 6).

Table 6. Calculated Propulsive Properties of the Positive Detonation Energy Compounds as Monopropellants

entry	CCT (K)	I_{sp} (s)	I_{vac} (s)	c^*
Na_2N_8	2680	218	229	1356
MgN_4	1541	151	166	901
AlN_4	2617	189	209	1127

These data include combustion chamber temperature (CCT), specific impulse (I_{sp}), vacuum specific impulse (I_{vac}) and characteristic velocity (c^*). Again, all of these salts are inferior to conventional explosives such as RDX in their propulsion characteristics.

4. CONCLUSIONS

In summary, we have performed a comprehensive theoretical study of possible forms of nitrogen N_4 as both the pure allotrope and its alkali, alkaline earth metal and aluminum salts. Thus, we can safely conclude that *syn*-N_4^{2-} anions cannot be achieved at ambient pressure. Obviously, *catena*-polyanions N_4^{2-} can exist in extremes, and their stability domain at low pressures still remains an enigma. Conversely, *syn*-N_4^{4-} anions, as it has already shown experimentally[34] and supported theoretically in the present work, may appear to be widely available at ambient conditions with other metal cations, beyond Mg_2N_4. Therefore, if synthesized these can become the youngest generation in the family of nitrogen salts with its "aged" azides and "adult" pentazolates, which, nevertheless, still continue to acquire new members.[67,77,78]

Remarkably, we have found in this work that the cyclic form of nitrogen *c*-N_4 (tetrazete) and its alkali and alkaline earth metal salts are also thermally, dynamically, and mechanically stable at ambient pressure. Moreover, *c*-N_4^{x-} anions are available in a wide ranges of oxidation states (when x = 1, 2, and 3). This fact can dramatically change strategies of synthesis of the tetranitrogen units in order to obtain its cyclic form. We have shown that by varying both metal and stoichiometry, one can obtain salts with a wide range of properties: band gap (1−5 eV), bulk modulus (44−196 GPa), enthalpy of formation (from −21

https://doi.org/10.1021/acs.jpcc.0c11425
J. Phys. Chem. C 2021, 125, 7368−7377

to 660 kJ mol^{-1}), and so forth. The latter values for the studied compounds are not so high and are comparable or even lower than that for other synthesized energetic materials, for example, 1,1′-azobis(3,5-diazido-1,2,4-triazole) C_4N_{20}.[79] Thus, Na_2N_8 and C_4N_{20} have enthalpies of formation equal 66.0 and 89.6 kJ mol^{-1} $atom^{-1}$, respectively. Therefore, one can conclude that the studied salts are in the achievable energetic region.

The power of cutting-edge computation methods already proved its crucial role in the guidance of experimental studies, like in the case of cg-N (12 years from prediction to discovery), *cyclo*-N_5^- (15 years from prediction to discovery), or N_8 (4 years from prediction to discovery). Thus, we hope this work inspires experimentalists to find synthetic routes to metal salts of *c*-N_4^{x-} anions. This will significantly expand our understanding of the possible forms of nitrogen existence in nature and, obviously, provides novel materials for various practical applications.

■ ASSOCIATED CONTENT

Supporting Information

The Supporting Information is available free of charge at https://pubs.acs.org/doi/10.1021/acs.jpcc.0c11425.

Crystal packing, fractional coordinates, critical points and paths, the Brillouin zone integration schemes, elastic stiffness and compliance constants, IR and Raman spectra, band structures and partial density of states, the enthalpy of formation calculation schemes, thermodynamic properties, and NASA coefficients (PDF)

■ AUTHOR INFORMATION

Corresponding Author

Sergey V. Bondarchuk − *Department of Chemistry and Nanomaterials Science, Bogdan Khmelnitsky Cherkasy National University, 18031 Cherkasy, Ukraine;* orcid.org/0000-0002-3545-0736; Phone: (+3) 80472 37-65-76; Email: bondchem@cdu.edu.ua; Fax: (+3) 80472 37-21-42

Complete contact information is available at: https://pubs.acs.org/10.1021/acs.jpcc.0c11425

Notes

The author declares no competing financial interest.

■ ACKNOWLEDGMENTS

This work was supported by the Ministry of Education and Science of Ukraine, Research Fund (Grant 0117U003908).

■ REFERENCES

(1) Klapötke, T. M. *Chemistry of High-Energy Materials*, 5th ed.; De Gruyter: Berlin, 2019; pp 283−299.
(2) Dobrynin, D.; Rakhmanov, R.; Fridman, A. Nanosecond-Pulsed Discharge in Liquid Nitrogen: Optical Characterization and Production of an Energetic Non-Molecular Form of Nitrogen-Rich Material. *J. Phys. D: Appl. Phys.* **2019**, *52*, 39LT01.
(3) Eremets, M. I.; Gavriliuk, A. G.; Trojan, I. A.; Dzivenko, D. A.; Boehler, R. Single-bonded cubic form of nitrogen. *Nat. Mater.* **2004**, *3*, 558−563.
(4) Tomasino, D.; Kim, M.; Smith, J.; Yoo, C.-S. Pressure-Induced Symmetry-Lowering Transition in Dense Nitrogen to Layered Polymeric Nitrogen (LP-N) with Colossal Raman Intensity. *Phys. Rev. Lett.* **2014**, *113*, 205502.
(5) Laniel, D.; Geneste, G.; Weck, G.; Mezouar, M.; Loubeyre, P. Hexagonal Layered Polymeric Nitrogen Phase Synthesized near 250 GPa. *Phys. Rev. Lett.* **2019**, *122*, 066001.
(6) Wang, H.; Eremets, M. I.; Troyan, I.; Liu, H.; Ma, Y.; Vereecken, L. Nitrogen Backbone Oligomers. *Sci. Rep.* **2015**, *5*, 13239.
(7) Bykov, M.; Bykova, E.; Koemets, E.; Fedotenko, T.; Aprilis, G.; Glazyrin, K.; Liermann, H.-P.; Ponomareva, A. V.; Tidholm, J.; Tasnádi, F.; et al. High-Pressure Synthesis of a Nitrogen-Rich Inclusion Compound $ReN_8 \bullet xN_2$ with Conjugated Polymeric Nitrogen Chains. *Angew. Chem., Int. Ed.* **2018**, *57*, 9048−9053.
(8) Duwal, S.; Ryu, Y.-J.; Kim, M.; Yoo, C.-S.; Bang, S.; Kim, K.; Hwi Hur, N. Transformation of Hydrazinium Azide to Molecular N_8 at 40 GPa. *J. Chem. Phys.* **2018**, *148*, 134310.
(9) Wu, Z.; Benchafia, E. M.; Iqbal, Z.; Wang, X. N_8^- Polynitrogen Stabilized on Multi-Wall Carbon Nanotubes for Oxygen-Reduction Reactions at Ambient Conditions. *Angew. Chem., Int. Ed.* **2014**, *53*, 12555−12559.
(10) Zhang, C.; Sun, C.; Hu, B.; Yu, C.; Lu, M. Synthesis and Characterization of the Pentazolate Anion cyclo-N_5^- in $(N_5)_6(H_3O)_3(NH_4)_4Cl$. *Science* **2017**, *355*, 374−376.
(11) Xu, Y.; Wang, Q.; Shen, C.; Lin, Q.; Wang, P.; Lu, M. A Series of Energetic Metal Pentazolate Hydrates. *Nature* **2017**, *549*, 78−81.
(12) Laniel, D.; Weck, G.; Gaiffe, G.; Garbarino, G.; Loubeyre, P. High-Pressure Synthesized Lithium Pentazolate Compound Metastable under Ambient Conditions. *J. Phys. Chem. Lett.* **2018**, *9*, 1600−1604.
(13) Benchafia, E. M.; Yao, Z.; Yuan, G.; Chou, T.; Piao, H.; Wang, X.; Iqbal, Z. Cubic Gauche Polymeric Nitrogen under Ambient Conditions. *Nat. Commun.* **2017**, *8*, 930.
(14) Bondarchuk, S. V. Bipentazole (N_{10}): A Low-Energy Molecular Nitrogen Allotrope with High Intrinsic Stability. *J. Phys. Chem. Lett.* **2020**, *11*, 5544−5548.
(15) Liu, S.; Zhao, L.; Yao, M.; Miao, M.; Liu, B. Novel All-Nitrogen Molecular Crystals of Aromatic N_{10}. *Adv. Sci.* **2020**, *10*, 1902320.
(16) Mailhiot, C.; Yang, L. H.; McMahan, A. K. Polymeric nitrogen. *Phys. Rev. B: Condens. Matter Mater. Phys.* **1992**, *46*, 14419−14435.
(17) Hirshberg, B.; Gerber, R. B.; Krylov, A. I. Calculations Predict a Stable Molecular Crystal of N_8. *Nat. Chem.* **2014**, *6*, 52−56.
(18) Bondarchuk, S. V. Beyond Molecular Nitrogen: Revelation of Two Ambient-Pressure Metastable Single- and Double-Bonded Nitrogen Allotropes Built from Three-Membered Rings. *Phys. Chem. Chem. Phys.* **2019**, *21*, 22930−22938.
(19) Bondarchuk, S. V.; Minaev, B. F. Super High-Energy Density Single-Bonded Trigonal Nitrogen AllotropeA Chemical Twin of the Cubic Gauche Form of Nitrogen. *Phys. Chem. Chem. Phys.* **2017**, *19*, 6698−6706.
(20) Bondarchuk, S. V.; Minaev, B. F. Two-Dimensional Honeycomb (A7) and Zigzag Sheet (ZS) Type Nitrogen Monolayers. A First Principles Study of Structural, Electronic, Spectral, and Mechanical Properties. *Comput. Mater. Sci.* **2017**, *133*, 122−129.
(21) Miao, M.; Sun, Y.; Zurek, E.; Lin, H. Chemistry under High Pressure. *Nat. Rev. Chem.* **2020**, *4*, 508−527.
(22) Glukhovtsev, M. N.; Jiao, H.; Schleyer, P. v. R. Besides N_2, What Is the Most Stable Molecule Composed Only of Nitrogen Atoms? *Inorg. Chem.* **1996**, *35*, 7124−7133.
(23) Ajith Perera, S.; Bartlett, R. J. Coupled-Cluster Calculations of Raman Intensities and their Application to N_4 and N_5^-. *Chem. Phys. Lett.* **1999**, *314*, 381−387.
(24) Rennie, E. E.; Mayer, P. M. Confirmation of the "Long-Lived" Tetra-Nitrogen (N_4) Molecule Using Neutralization-Reionization Mass Spectrometry and ab initio Calculations. *J. Chem. Phys.* **2004**, *120*, 10561.
(25) Cacace, F.; de Petris, G.; Troiani, A. Experimental Detection of Tetranitrogen. *Science* **2002**, *295*, 480−481.
(26) Cacace, F. From N_2 and O_2 to N_4 and O_4: Pneumatic Chemistry in the 21st Century. *Chem. - Eur. J.* **2002**, *8*, 3838−3847.
(27) Nguyen, M. T.; Nguyen, T. L.; Mebel, A. M.; Flammang, R. Azido-Nitrene Is Probably the N_4 Molecule Observed in Mass Spectrometric Experiments. *J. Phys. Chem. A* **2003**, *107*, 5452−5460.
(28) Nguyen, M. T. Polynitrogen compounds: 1. Structure and stability of N_4 and N_5 systems. *Coord. Chem. Rev.* **2003**, *244*, 93−113.

(29) Peng, F.; Han, Y.; Liu, H.; Yao, Y. Exotic Stable Cesium Polynitrides at High Pressure. *Sci. Rep.* **2015**, *5*, 16902.
(30) Zhu, S.; Peng, F.; Liu, H.; Majumdar, A.; Gao, T.; Yao, Y. Stable Calcium Nitrides at Ambient and High Pressures. *Inorg. Chem.* **2016**, *55*, 7550−7555.
(31) Shen, Y.; Oganov, A. R.; Qian, G.; Zhang, J.; Dong, H.; Zhu, Q.; Zhou, Z. Novel Lithium-Nitrogen Compounds at Ambient and High Pressures. *Sci. Rep.* **2015**, *5*, 14204.
(32) Huang, B.; Frapper, G. Barium-Nitrogen Phases Under Pressure: Emergence of Structural Diversity and Nitrogen-Rich Compounds. *Chem. Mater.* **2018**, *30*, 7623−7636.
(33) Yu, S.; Huang, B.; Zeng, Q.; Oganov, A. R.; Zhang, L.; Frapper, G. Emergence of Novel Polynitrogen Molecule-like Species, Covalent Chains, and Layers in Magnesium-Nitrogen Mg_xN_y Phases under High Pressure. *J. Phys. Chem. C* **2017**, *121*, 11037−11046.
(34) Laniel, D.; Winkler, B.; Koemets, E.; Fedotenko, T.; Bykov, M.; Bykova, E.; Dubrovinsky, L.; Dubrovinskaia, N. Synthesis of Magnesium-Nitrogen Salts of Polynitrogen Anions. *Nat. Commun.* **2019**, *10*, 451.
(35) Bykov, M.; Bykova, E.; Aprilis, G.; Glazyrin, K.; Koemets, E.; Chuvashova, I.; Kupenko, I.; McCammon, C.; Mezouar, M.; Prakapenka, V.; Liermann, H.-P.; Tasnádi, F.; Ponomareva, A. V.; Abrikosov, I. A.; Dubrovinskaia, N.; Dubrovinsky, L. Fe-N System at High Pressure Reveals a Compound Featuring Polymeric Nitrogen Chains. *Nat. Commun.* **2018**, *9*, 2756.
(36) Malyi, O. I.; Sopiha, K. V.; Persson, C. Energy, Phonon, and Dynamic Stability Criteria of Two-Dimensional Materials. *ACS Appl. Mater. Interfaces* **2019**, *11* (28), 24876−24884.
(37) Steele, B. A.; Oleynik, I. I. Computational Discovery of New High-Nitrogen Energetic Materials. In *Computational Approaches for Chemistry Under Extreme Conditions*; Goldman, N., Eds.; Springer, 2019; Vol. *28*, pp 25−52.
(38) *Materials Studio 2017*; Dassault Systèmes BIOVIA, San Diego, CA, 2016.
(39) Chai, J.-D.; Head-Gordon, M. Long-range corrected hybrid density functionals with damped atom-atom dispersion corrections. *Phys. Chem. Chem. Phys.* **2008**, *10*, 6615−6620.
(40) Hehre, W. J.; Radom, L.; Schleyer, P. v. R.; Pople, J. A. *Ab Initio Molecular Orbital Theory*; Wiley: New York, 1986.
(41) Frisch, M. J.; Trucks, G. W.; Schlegel, H. B.; Scuseria, G. E.; Robb, M. A.; Cheeseman, J. R.; Scalmani, G.; Barone, V.; Mennucci, B.; Petersson, G. A. et al. *Gaussian 09*, Revision A.02; Gaussian, Inc.: Wallingford, CT, 2009.
(42) Rappé, A. K.; Casewit, C. J.; Colwell, K. S.; Goddard, W. A.; Skiff, W. M. UFF, a full periodic table force field for molecular mechanics and molecular dynamics simulations. *J. Am. Chem. Soc.* **1992**, *114*, 10024−10035.
(43) CSD Space Group Statistics - Space Group Number Ordering 2020. https://www.ccdc.cam.ac.uk/ (accessed Aug 27, 2020).
(44) Bondarchuk, S. V. CarNit4 - A new polymeric energetic material based on poly(1,5-tetrazolediyl). *Polymer* **2020**, *186*, 122048.
(45) Bondarchuk, S. V. Modeling of Explosives: 1,4,2,3,5,6-Dioxatetrazinane as a New Green Energetic Material with Enhanced Performance. *J. Phys. Chem. Solids* **2020**, *142*, 109458.
(46) Clark, S. J.; Segall, M. D.; Pickard, C. J.; Hasnip, P. J.; Probert, M. J.; Refson, K.; Payne, M. C. First principles methods using CASTEP. *Z. Kristallogr. - Cryst. Mater.* **2005**, *220*, 567−570.
(47) Perdew, J. P.; Burke, K.; Ernzerhof, M. Generalized Gradient Approximation Made Simple. *Phys. Rev. Lett.* **1996**, *77*, 3865−3868.
(48) Heyd, J.; Scuseria, G. Efficient hybrid density functional calculations in solids: Assessment of the Heyd-Scuseria-Ernzerhof screened Coulomb hybrid functional. *J. Chem. Phys.* **2004**, *121*, 1187−1192.
(49) Bondarchuk, S. V.; Minaev, B. F. Two Isomeric Solid Carbon Nitrides With 1:1 Stoichiometry Which Exhibit Strong Mechanical Anisotropy. *New J. Chem.* **2017**, *41*, 13140−13148.
(50) Grimme, S. Semiempirical GGA-type Density Functional Constructed with a Long-Range Dispersion Correction. *J. Comput. Chem.* **2006**, *27*, 1787−1799.
(51) Delley, B. From Molecules to Solids with the $DMol^3$ Approach. *J. Chem. Phys.* **2000**, *113*, 7756−7764.
(52) Keith, T. A. *AIMAll*, Version 10.07.25; TK Gristmill Software: Overland Park, KS, 2010. Available at www.aim.tkgristmill.com.
(53) Nyman, J.; Day, G. M. Static and Lattice Vibrational Energy Differences between Polymorphs. *CrystEngComm* **2015**, *17*, 5154−5165.
(54) Bondarchuk, S. V. Magic of Numbers: A Guide for Preliminary Estimation of the Detonation Performance of C-H-N-O Explosives Based on Empirical Formulas. *Ind. Eng. Chem. Res.* **2021**, *60*, 1952−1961.
(55) Cremer, D.; Kraka, E. A Description of the Chemical Bond in Terms of Local Properties of Electron Density and Energy. *Croat. Chem. Acta* **1984**, *56*, 1259−1281.
(56) Bondarchuk, S. V.; Minaev, B. F.; Fesak, A. Yu. Theoretical Study of the Triplet State Aryl Cations Recombination: A Possible Route to Unusually Stable Doubly Charged Biphenyl Cations. *Int. J. Quantum Chem.* **2013**, *113*, 2580−2588.
(57) Jeffrey, G. A.; Parry, G. S. Crystal Structure of Aluminum Nitride. *J. Chem. Phys.* **1955**, *23*, 406.
(58) Morkoç, H. *Handbook of Nitride Semiconductors and Devices. Vol. 1: Materials Properties, Physics and Growth*; Wiley-VCH Verlag GmbH: Weinheim, 2008; pp 140−141.
(59) Geier, J.; Grützmacher, H.; Exner, K.; Prinzbach, H. In-Plane Bishomoaromaticity in Tetranitrogen Dianions: Solid-State, Solution, and Electronic Structures. *Angew. Chem., Int. Ed.* **2005**, *44*, 2433−2437.
(60) Bauzá, A.; Quiñonero, D.; Deyà, P. M.; Frontera, A. Estimating Ring Strain Energies in Small Carbocycles by Means of the Bader's Theory of 'Atoms-in-Molecules'. *Chem. Phys. Lett.* **2012**, *536*, 165−169.
(61) Xu, Y.; Tian, L.; Li, D.; Wang, P.; Lu, M. A Series of Energetic cyclo-Pentazolate Salts: Rapid Synthesis, Characterization, and Promising Performance. *J. Mater. Chem. A* **2019**, *7*, 12468−12479.
(62) Hoesch, L.; Leuenberger, C.; Hilpert, H.; Dreiding, A. S. Erste Beispiele: 2, 3-Dialkyl-triaziridin-1-carbonsäurealkylester. *Helv. Chim. Acta* **1982**, *65*, 2682−2696.
(63) Camp, D.; Campitelli, M.; Hanson, G. R.; Jenkins, I. D. Formation of an Unusual Four-Membered Nitrogen Ring (Tetrazetidine) Radical Cation. *J. Am. Chem. Soc.* **2012**, *134*, 16188−16196.
(64) Curtarolo, S.; Setyawan, W.; Hart, G. L. W.; Jahnatek, M.; Chepulskii, R. V.; Taylor, R. H.; Wang, S.; Xue, J.; Yang, K.; Levy, O.; et al. AFLOW: An Automatic Framework for High-Throughput Materials Discovery. *Comput. Mater. Sci.* **2012**, *58*, 218−226.
(65) Mouhat, F.; Coudert, F.-X. Necessary and Sufficient Elastic Stability Conditions in Various Crystal Systems. *Phys. Rev. B: Condens. Matter Mater. Phys.* **2014**, *90*, 224104.
(66) Bondarchuk, S. V. Theoretical Evaluation of Hexazinane as a Basic Component of Nitrogen-Rich Energetic Onium Salts. *Mol. Syst. Des. Eng.* **2020**, *5*, 1003−1011.
(67) Vaidya, S. N.; Kennedy, G. C. Compressibility of 18 Molecular Organic Solids to 45 kbar. *J. Chem. Phys.* **1971**, *55*, 987−992.
(68) Vaidya, S. N.; Kennedy, G. C. Compressibility of 27 Halides to 45 kbar. *J. Phys. Chem. Solids* **1971**, *32*, 951−964.
(69) NIST Chemistry WebBook. https://webbook.nist.gov/chemistry/ (accessed Aug 27, 2020).
(70) Gray, P.; Waddington, T. C. Thermochemistry and Reactivity of the Azides. I. Thermochemistry of the Inorganic Azides. *Proc. R. Soc. London A* **1956**, *235*, 106−119.
(71) Xu, Y.; Tian, L.; Li, D.; Wang, P.; Lu, M. A Series of Energetic cyclo-Pentazolate Salts: Rapid Synthesis, Characterization, and Promising Performance. *J. Mater. Chem. A* **2019**, *7*, 12468−12479.
(72) Wang, Y.; Zhang, J.; Su, H.; Li, S.; Zhang, S.; Pang, S. A Simple Method for the Prediction of the Detonation Performances of Metal-Containing Explosives. *J. Phys. Chem. A* **2014**, *118*, 4575−4581.
(73) Gordon, S.; McBride, B. J. Computer Program for Calculation of Complex Chemical Equilibrium Compositions and Applications. *I. Analysis*; NASA Reference Publication 1311; NASA: Cleveland, OH, 1994.
(74) Bondarchuk, S. V.; Yefimenko, N. A. An Algorithm for Evaluation of Potential Hazards in Research and Development of New Energetic

https://doi.org/10.1021/acs.jpcc.0c11425
J. Phys. Chem. C 2021, 125, 7368−7377

Materials in Terms of their Detonation and Ballistic Profiles. *Propellants, Explos., Pyrotech.* **2018**, *43*, 818−824.

(75) McBride, B. J.; Zehe, M. J.; Gordon, S. *NASA Glenn Coefficients for Calculating Thermodynamic Properties of Individual Species*. Glenn Research Center, Cleveland, OH, 2002. (OhioNASA/TP-2002−211556).

(76) Yue, P.; Long, X.; Jiang, X.; Zhang, Z. Only Numerical Modeling of Detonation Properties for Some Metal Azides. *Propellants Explos. Pyrotech.* **2019**, *44*, 1−8.

(77) Tian, L.; Xu, Y.; Lin, Q.; Wang, P.; Lu, M. Syntheses of Energetic cyclo-Pentazolate Salts. *Chem.—Asian J.* **2019**, *14*, 2877−2882.

(78) Zhao, G.; Kumar, D.; Hu, L.; Shreeve, J. M. A Safe and Scaled-Up Route to Inert Ammonia Oxide Hydroxylammonium Azide ($H_7N_5O_2$), Hydrazinium Azide (H_5N_5), and Ammonium Azide (H_4N_4). *ACS Appl. Energy Mater.* **2019**, *2*, 6919−6923.

(79) Li, Y.; Wang, B.; Chang, P.; Hu, J.; Chen, T.; Wang, Y.; Wang, B. Novel Catenated N_6 Energetic Compounds Based on Substituted 1,2,4-Triazoles: Synthesis, Structures and Properties. *RSC Adv.* **2018**, *8*, 13755−13763.

https://doi.org/10.1021/acs.jpcc.0c11425
J. Phys. Chem. C 2021, 125, 7368−7377